

## Interaction between thermal phonons and dislocations in LiF

E. P. Roth\* and A. C. Anderson

*Department of Physics and Materials Research Laboratory, University of Illinois, Urbana, Illinois 61801*

(Received 20 March 1979)

All measurements of thermal conductivity and ballistic phonon propagation in crystals of deformed LiF over the temperature range 0.03–25 K are consistent with an interpretation in which the slow transverse phonons are scattered with much greater probability by dislocations than are fast transverse phonons. The scattering is too strong to be explained by static mechanisms of phonon-dislocation interaction, but is in rough agreement with a vibration-string mechanism. The present string model does not, however, provide the quantitative details observed experimentally.

### I. INTRODUCTION

In a previous publication,<sup>1</sup> the interaction between thermal phonons and edge dislocations in LiF was investigated through measurements of thermal conductivity  $\kappa$  and ballistic phonon propagation. It was argued that a strong, frequency-dependent, resonant interaction occurred between edge dislocations and phonons of the slow transverse mode. The resonance frequency of the dislocations could be increased by adding pinning points created by  $\gamma$  irradiation. Fully pinned, sessile edge dislocations scattered phonons only weakly, well below the resolution of the measurements.

In the present paper, we provide additional evidence which supports the conclusions of Ref. 1. In addition, we extend the measurements to include more complex configurations of dislocations, and to include thermal phonons of much higher frequency. The results are compared with theoretical calculations, and with measurements obtained in other laboratories. In brief, we believe the strong mode-dependent scattering extends to very high phonon frequencies corresponding to  $\hbar\omega/3.8 \text{ k} \approx 10 \text{ K}$ .

### II. EXPERIMENTAL DETAILS

The original crystals were Harshaw<sup>2</sup> optical-grade LiF having dimensions of  $0.5 \times 0.5 \times 5 \text{ cm}^3$ . The sample labeled *D* retained these dimensions. Other crystals, labeled *A*, *B*, *C*, were cut to  $0.15 \times 0.20 \times 5 \text{ cm}^3$ . The long axis of each crystal was directed along  $[110]$ , and the sides were oriented to  $[\bar{1}10]$  and  $[001]$ . After the initial measurement of  $\kappa$ , each sample was deformed by either shearing or bending at room temperature. Shearing produced an  $\approx 0.1$ -cm-thick wall of dislocations as indicated in Fig. 1(a). Additional details are given in Ref. 1. Bending was produced in a three-point jig; the resulting strain is depicted in Fig. 1(b).

Thermal conductivities were measured using the

arrangement of Fig. 1(c). Measurements were first made in the undeformed, annealed state. Samples deformed by shearing used three thermometers as shown in Fig. 1(c) with the sheared region lying between thermometers *A* and *B*. Thermometers *B* and *C* measured the "background" region which was not intentionally deformed. For samples deformed by bending, only thermometers *A* and *C* were used in the deformed region of the sample. All samples were remeasured after exposure to a succession of 0.66-Mev  $\gamma$  irradiations from a  $^{137}\text{Cs}$  source.<sup>3</sup>

Temperatures below  $\approx 3 \text{ K}$  for all experiments were derived from a set of superconducting fixed points<sup>4</sup> using a magnetic thermometer<sup>5</sup> for extrapolation and interpolation. Accuracy was  $\approx 1\%$ . Above 3 K the temperatures were obtained from a calibrated germanium resistance thermometer which was consistent with the higher temperature fixed points.

In Ref. 1 the surfaces of all LiF samples were intentionally abraided to cause nonspecular boundary scattering of thermal phonons and hence provide a known or reference mean free path. In the present measurements the surfaces were mechanically and chemically polished to avoid nonspecular scattering and hence provide a greater sensitivity to the internal scattering mechanisms of interest. This approach was highly successful below  $\approx 0.3 \text{ K}$ ; at 0.1 K the phonons were reflected roughly ten times from the surfaces before encountering a nonspecular scattering. In retrospect, however, polishing of the sample surfaces was not wise since the remanent, nonspecular scattering was sensitive to sample history and not readily reproducible. For this reason sample *D* was lightly abraided with air-borne powder.

The history-dependent behavior of the nonspecular surface scattering can be seen in Fig. 2 for the background region of sample *A*. Specular reflection increases with polishing, with etching, or with  $\gamma$  irradiation as observed previously by

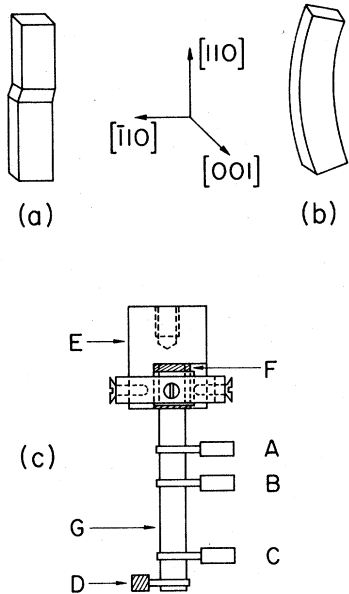


FIG. 1. Sample orientation and methods of deformation; (a) sheared along  $[110]$  direction; (b), bent about  $[001]$  axis; (c), typical experimental arrangement for thermal-conductivity measurements; A, B, C, carbon or germanium resistance thermometers; D, electrical heater; E, copper holder; F, thin indium foil; G, sample.

others.<sup>6</sup> However, for  $T \geq 0.4$  K nonspecular reflection is nearly independent of sample history and close to the Casimir limit,<sup>6</sup> i.e., nearly all phonon scattering from the surfaces is nonspecular. The Casimir limit is represented by the arrow in Fig. 2, and has been corrected for end effects<sup>7</sup> and phonon focusing.<sup>8</sup> Hence, problems as-

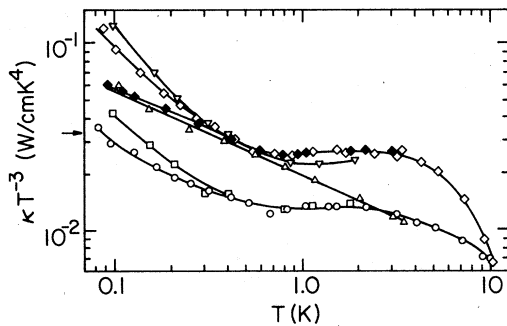


FIG. 2. Thermal conductivity of sheared LiF sample A of  $\approx 0.15 \times 0.2$ -cm<sup>2</sup> cross section, divided by  $T^3$  to allow vertical expansion of data.  $\blacklozenge$ , annealed and polished sample before deformation. After deformation and etching:  $\circ$ , undeformed background region;  $\nabla$ , background after 720 R of  $\gamma$  irradiation;  $\circ$ , sheared region;  $\square$ , sheared region after 720 R;  $\blacktriangle$ , sheared region after 180 000 R. Arrow represents value of  $\kappa T^{-3}$  if no phonons were specularly reflected from the crystal surfaces.

sociated with history-dependent boundary scattering are limited to  $T \leq 0.3$  K.

The dislocation densities in the deformed regions of the samples were estimated from etch-pit counts assuming a one-to-one correspondence.<sup>9</sup> Etch-pit counts were obtained in both optical and scanning-electron microscopes from the sample faces as well as an internal (100) plane exposed by cleaving each sample at the conclusion of the  $\kappa$  measurements. Primarily edge dislocations intersect the (001) sample faces while, from the orientation of the glide bands, it appeared that roughly equal numbers of screw and edge dislocations intersected the (100) plane.

Sample A contained a dislocation density of  $3 \times 10^7$  cm<sup>-2</sup> in the sheared region of 0.1-cm width [Fig. 1(a)]. These were primarily edge dislocation since only  $\approx 6 \times 10^5$  cm<sup>-2</sup> intersected the cleaved (100) plane, which was the same density as in the as-received material.

Sample B was bent through an angle of  $40^\circ$  about a 4.6-cm radius and contained a dislocation density of  $\approx 2 \times 10^7$  cm<sup>-2</sup> on both the (001) and (100) planes. We therefore use an average density in the bent region of  $4 \times 10^7$  cm<sup>-2</sup> effective in scattering thermal phonons while recognizing that perhaps  $\frac{1}{4}$  of the total are screw dislocations.

Sample C was bent to a larger radius of  $\approx 20$  cm and contained  $5 \times 10^6$  cm<sup>-2</sup> intersecting one plane. As for sample B, we take the average density normal to a given direction to be  $10^7$  cm<sup>-2</sup>.

Sample D, the bent sample of larger cross section, also contained a density of  $5 \times 10^6$  cm<sup>-2</sup> intersecting one plane. Again we take the effective average to be  $10^7$  cm<sup>-2</sup>, recognizing that perhaps  $\frac{1}{4}$  are screw dislocations.

The dislocation densities measured on the (001) surfaces are consistent with the minimum density of edge dislocations calculated from the radius of curvature of a deformed sample.

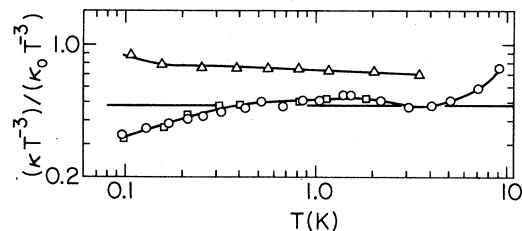


FIG. 3. Ratio of  $\kappa T^{-3}$  in the sheared region of sample A divided by  $\kappa_0 T^{-3}$  of the undeformed region. Symbols same as Fig. 2. A value of 1.0 would indicate no additional phonon scattering resulting from deformation. The horizontal line represents the expected ratio if only the slow transverse phonons were strongly scattered.

### III. RESULTS AND DISCUSSION

In this section we first discuss the experimental results using only the Debye model of thermal transport, then compare our results with earlier measurements on LiF in other laboratories, and finally compare the experimental results with available theories of phonon-dislocation interactions.

#### A. Qualitative discussion of data

The thermal conductivities of samples *A*, *B*, and *D* are shown in Figs. 2, 4, and 6. The data have been divided by  $T^3$  to allow expansion of the vertical scale so that changes in  $\kappa$  with deformation and irradiation may be seen more conveniently. The decrease in  $\kappa T^{-3}$  near 10 K simply indicates that the peak in  $\kappa$  vs  $T$  lies near 20 K as is typical of LiF crystals having 0.2–0.5-cm lateral dimensions. The increase in  $\kappa T^{-3}$  below  $\approx 0.3$  K for undeformed samples is largely due to increased specular scattering from the sample surfaces as discussed in Sec. II, and therefore the data for  $T < 0.3$  K are less useful in the present discussion.

In Figs. 3, 5, and 7 the  $\kappa T^{-3}$  data have been divided by  $\kappa_0 T^{-3}$  measured in the background region (for sample *A*) or before deformation (for samples *B*, *C*, and *D*). A value of 1.0 in a plot of  $\kappa T^{-3}/\kappa_0 T^{-3}$  would indicate no change in phonon scattering relative to the undeformed crystal.

Four important facts are available from Figs. 2–7. *First*, the ratio of  $\kappa T^{-3}/\kappa_0 T^{-3}$  for the sheared sample is the same as measured in Ref. 1 for samples with the same dislocation density but a factor of 2 larger lateral dimensions. In other words, the magnitude of the thermal conductivity of *deformed* LiF is proportional to the size of the sample. This indicates that even after the sample

is sheared, some fraction of the phonons are still scattered primarily by the surfaces of the sample, i.e., some fraction of the phonons retain a long mean free path. This is also evident in comparing the two bent samples *C* ( $\times$  in Fig. 5) and *D* (Fig. 7) which have the same dislocation density but differ by a factor of 2 in lateral dimensions.

*Second*, the ratios of  $\kappa T^{-3}/\kappa_0 T^{-3}$  for samples *B* and *C* (Fig. 5) are the same. These two crystals had the same dimensions, but *B* had a larger dislocation density. Hence the ratio of  $\kappa T^{-3}/\kappa_0 T^{-3}$  of bent samples is independent of the number of dislocations present, just as observed in Ref. 1 for sheared samples. This behavior indicates that those phonons which are scattered by dislocations are scattered sufficiently strongly that they make essentially *no* contribution to thermal transport in the present samples. To observe the magnitude of this scattering would require the introduction of a fresh dislocation density of  $\ll 10^7$  cm<sup>-2</sup>. Our attempts to do this failed.

*Third*, from Figs. 3, 5, and 7 it may be noted that successive exposures to  $\gamma$  irradiation restores the thermal conductivity to nearly the pre-deformation magnitude. The effect starts at low temperatures and progresses to higher temperatures as the total irradiation dosage is increased. Since the dislocations are still present, these results imply that the phonon-dislocation interaction is dynamic or resonant in character and that irradiation progressively pins the dislocations so that they become sessile. The lengths of the segments of a dislocation which can move in the stress field of an incident thermal phonon are reduced with increased irradiation, i.e., the frequency of the resonant interaction is increased. The same behavior was observed more definitely in Ref. 1 since the problems with specular reflections below  $\approx 0.3$  K were avoided.

*Fourth*, the strong phonon scattering of a fraction of the total phonon population persists to tem-

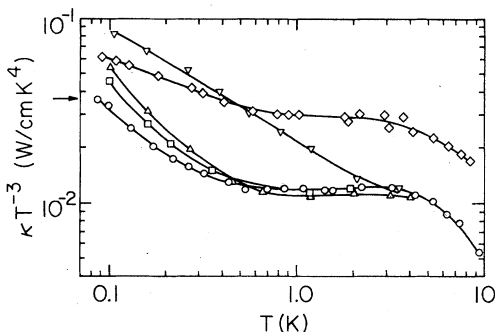


FIG. 4. Thermal conductivity of bent sample *B* of  $0.15 \times 0.2$ -cm<sup>2</sup> cross section, divided by  $T^3$ .  $\diamond$ , deformed annealed and polished sample. After deformation and etching:  $\circ$ , bent region;  $\square$ , 720 R of  $\gamma$  irradiation;  $\triangle$ , 2100 R;  $\nabla$ , 180 000 R. The Casimir limit is indicated by an arrow.

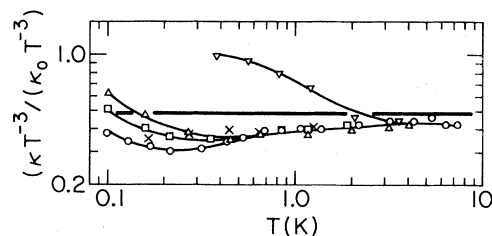


FIG. 5. Ratio of  $\kappa T^{-3}$  of bent sample *B* divided by  $\kappa_0 T^{-3}$  of crystal prior to deformation. The horizontal line represents the expected ratio if only slow transverse phonons were strongly scattered. Symbols same as Fig. 4, except  $\times$ : bent sample *C* of same cross section, but a factor of 6 smaller dislocation density.

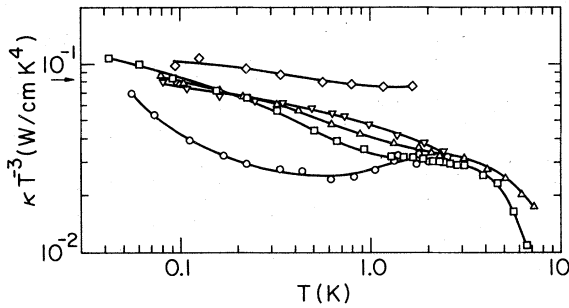


FIG. 6. Thermal conductivity of bent crystal *D* of larger ( $0.5 \times 0.5 \text{ cm}^2$ ) cross section, divided by  $T^3$ . Surfaces were lightly abraded to provide phonon boundary scattering as a reference mean free path. Some data are omitted for clarity.  $\diamond$ , undeformed annealed crystal. Deformed sample:  $\circ$ , bent region;  $\square$ , 40 000 R of  $\gamma$  irradiation;  $\triangle$ , 80 000 R;  $\nabla$ , 200 000 R. The arrow indicates the value of  $\kappa T^{-3}$  if no phonons were specularly reflected from the surfaces.

peratures at high as  $\approx 10 \text{ K}$  and, for the bent samples, perhaps higher. The  $\gamma$  irradiation appears incapable of removing this strong scattering for temperatures above  $\approx 3 \text{ K}$ . Hence the present data do not indicate whether phonon scattering from dislocations for  $T \geq 3 \text{ K}$  is by a resonant or static mechanism. It must be emphasized, however, that the size effect is present above  $2 \text{ K}$ , i.e., only some fraction of the phonons in our samples are strongly scattered by the dislocations. Another fraction have long mean free paths and are scattered by sample surfaces.

In Ref. 1 it was demonstrated directly through observation of ballistic phonon pulses that, near  $3.6 \text{ K}$  in sheared samples, only the slow transverse phonon mode was strongly scattered by edge dislocations. In Figs. 3, 5, and 7 the calculated ratio of  $\kappa T^{-3}/\kappa_0 T^{-3}$  assuming no transport by slow transverse phonons in the deformed crystals is indicated by the horizontal line. For the three bent samples, the measured  $\kappa T^{-3}/\kappa_0 T^{-3}$  is somewhat lower than this horizontal line, suggesting that a second phonon mode is being strongly scattered by the more complex dislocation configuration present in bent samples. This additional scattering in bent samples removes  $\approx 15\%$  of the total conductivity of the undeformed crystals, which suggests that the longitudinal mode may be involved. In this case, the fast transverse mode would have a mean free path limited only by boundary scattering and would account for essentially the entire heat transport in the bent samples.

In summary, we find that edge dislocations strongly scatter slow transverse phonons in LiF via a resonant interaction. In bent samples another fraction of the thermal phonons, possibly the

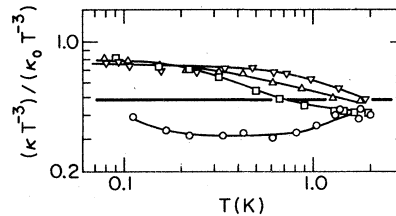


FIG. 7. Ratio of  $\kappa T^{-3}$  of bent sample *D*, of larger cross section, divided by  $\kappa_0 T^{-3}$  of the undeformed crystal. Symbols same as Fig. 6. The horizontal line represents the expected ratio if only slow transverse phonons were scattered strongly.

longitudinal branch, also interacts strongly with dislocations. The remaining fraction of phonons have mean free paths limited by the dimensions of the sample. Pinning the dislocations increases the frequency of the resonant interactions, but only for frequencies below  $\hbar\omega/3.8 \text{ k} \approx 3 \text{ K}$ .

#### B. Comparison with other data

The only data we are aware of for bent LiF crystals are from a single measurement above  $2 \text{ K}$  by Taylor *et al.*<sup>10</sup> for a sample containing a dislocation density of  $\approx 2 \times 10^7 \text{ cm}^{-2}$  based on an etch-pit count. Below  $\approx 4 \text{ K}$  the thermal conductivity varied as  $T^3$  and was reduced to  $\approx 35\%$  of the value for the undeformed sample, the same as the present measurements. Also a strong phonon scattering persisted in the deformed crystal to temperatures as high as  $25 \text{ K}$ , as for the present samples.

Most data available from the literature pertain to LiF samples of similar dimensions, but deformed by compression and measured only for temperatures  $\geq 2 \text{ K}$ . Both Sproull *et al.*<sup>11</sup> and Suzuki and Suzuki<sup>12</sup> equated the dislocation densities to etch-pit counts obtain on a single crystal plane. The results of both papers, which agree within a factor of 2, show for large deformation associated with dislocation densities of  $\geq 10^8 \text{ cm}^{-2}$  that the thermal conductivity *does* scale inversely with the density of dislocations. An angle-averaged dislocation density of  $\approx 6 \times 10^8 \text{ cm}^{-2}$  reduces  $\kappa$  near  $2 \text{ K}$  from  $\approx 1.4 \text{ W/cm K}$  to  $\approx 0.02 \text{ W/cm K}$ . This result, in which all phonon modes are scattered, is consistent with the conclusions presented in Sec. IIIA if we continue to assume that only a fraction of the phonons, possibly the fast transverse mode, provide essentially all the thermal transport. Scaling the scattering observed by Suzuki and Suzuki to the average dislocation density of  $4 \times 10^7 \text{ cm}^{-2}$  for our sample *B* would give  $\kappa \approx 0.3 \text{ W/cm K}$  at  $2 \text{ K}$ . However, in our sample having a thickness of  $\approx 0.15 \text{ cm}$ , boundary scattering limits  $\kappa$  to  $\approx 3 \times 10^{-2} \text{ W/cm K}$ . Hence the weakly scattered mode is

little affected by the presence of dislocations in our samples.

Suzuki and Suzuki<sup>12</sup> also pinned dislocations by partially annealing their samples. Above  $\approx 3$  K there was no change in the temperature dependence of  $\kappa$  after annealing, just as in our samples there was no change in temperature dependence with  $\gamma$  irradiation. In like manner, below 3 K there was a change in the temperature dependence of  $\kappa$  which suggested that the frequency of a resonant phonon-dislocation interaction was being increased with increased pinning.

Thus we find that the previous measurements are completely consistent with the present data and with the interpretation placed on the present data. We summarize these results here for use in Sec. III C. In deformed LiF, all phonons are scattered by dislocations, but the slow transverse mode is scattered much more strongly than the fast transverse mode. The frequency dependence of this scattering can be altered by pinning the dislocations. Since the longitudinal phonon mode normally contributes only  $\approx 14\%$  of thermal transport (versus  $\approx 53\%$  for slow transverse and  $\approx 33\%$  for fast transverse), it is not possible to determine if it is scattered weakly or strongly. The present data plus those from Ref. 1 suggest that the longitudinal mode is scattered rather strongly.

### C. Comparison with theoretical models

Theoretical scattering mechanisms can be divided into two general classes, namely, static scattering processes and dynamic or resonant scattering processes.

The static mechanism has been calculated explicitly for the three phonon modes in LiF and other materials by Kogure and Hiki,<sup>13</sup> who also summarize earlier calculations. They predict  $\kappa \propto T^2$ . While this calculation gives reasonable agreement for materials such as Si and Cu, it gives a scattering cross section a factor of  $10^2$ – $10^3$  too small to explain the LiF results even at temperatures above 10 K.

A calculation by Eckhardt and Wasserbäch<sup>14</sup> attempts to explain the  $T^3$  dependence of  $\kappa$  for bent LiF crystals in terms of a static scattering resulting from a spatial variation in crystal orientation. We have already demonstrated that the  $T^3$  behavior, when it occurs, is a result which depends on sample size, the fast transverse phonons are simply undergoing nonspecular boundary scattering. In the present measurements this  $T^3$  dependence occurs only between 0.3 and 3 K. In addition,  $\gamma$  irradiation does not remove the dislocations or change the variation in crystal orientation, but irradiation does erase the strong scat-

tering of phonons by dislocations in this  $T^3$  regime. Finally, the calculated scattering magnitude for this static mechanism is much too weak to explain our data.

The failure of static scattering models to explain the data on deformed LiF suggests that the strong scattering may be related to a dynamic process. Both Granato<sup>15,16</sup> and Ninomiya<sup>17,18</sup> have calculated the phonon scattering caused by the "fluttering" of a dislocation in the presence of a passing phonon. For simplicity we may visualize the dislocation as an elastic string. For a dislocation of infinite length the dislocation can be excited to some extent by a phonon of any frequency. If the dislocation, however, is pinned with an average<sup>19</sup> segment  $L_0$  free to flutter, only phonons having a frequency greater than some minimum value,  $\omega_0$ , can excite the dislocation. Ninomiya considers only the infinite dislocation, but the calculation can be adopted to dislocation segments of finite length by terminating<sup>1,12</sup> at a low-frequency limit  $\omega_0$  all integrations involving phonon scattering. Granato has shown that this approximation may underestimate the phonon scattering cross section for phonons having frequencies lying close to the dislocation resonance at  $\omega_0$ . Granato's vibrating string model has had considerable success in explaining the results of ultrasonic measurements.<sup>16</sup> As the phonon frequency is increased to the  $\approx 10^{12}$ -Hz range important in thermal transport near 10 K, the variation in effective mass<sup>20</sup> and line tension of the dislocation must be included explicitly in the calculations.<sup>16,18,21</sup>

A current problem with the vibrating string model is that the individual scattering cross sections for the three phonon modes from the two types of dislocations have not been calculated for all angles of incidence. The model gives only a rough magnitude for the thermal conductivity in the presence of dislocations. Of course, qualitative information on the relative scattering cross sections can be deduced from the Peach-Koehler relation.<sup>22</sup> Indeed, edge dislocations in LiF crystals oriented as in Fig. 1 should scatter the slow transverse mode most strongly.<sup>1,13</sup>

In comparing the vibrating string model with available data we first consider the freshly deformed samples for which  $\hbar\omega_0/3.8 \text{ k} \ll 5 \text{ K}$ . Then the measured mean free path of fast transverse phonons at 5 K is  $\approx 0.06 \text{ cm}$  for an angle-averaged dislocation density<sup>12</sup> of  $7 \times 10^8 \text{ cm}^{-2}$ . On the other hand, from our sample B (Fig. 4), the mean free path of slow transverse phonons is  $< 0.1 \text{ cm}$  for a dislocation density of  $4 \times 10^7 \text{ cm}^{-2}$ . Scaled to a density of  $7 \times 10^8 \text{ cm}^{-2}$ , the mean free path of slow transverse phonons would be  $< 0.006 \text{ cm}$ . The mean free path calculated using the string model

is  $\approx 0.02$  cm at 5 K. Hence the model predicts slightly too strong a scattering for the fast transverse mode near 5 K, but too weak a scattering for the slow transverse model.

It is also useful to make a comprehensive comparison with the data available at lower temperatures. Figure 8 reproduces part of the data from sample *D* (Fig. 6). The thermal conductivity of the undeformed sample was calculated using Callaway's model<sup>23</sup> with adjusted phonon scattering terms for boundaries, isotopes, umklapp processes, and normal phonon processes, and allowing for end effects and phonon focusing. Below  $\approx 3$  K only the boundary term is important; between 3 and 10 K the isotope term dominates. The boundary term agreed with the measured dimensions of the sample (between 0.3 and 3 K) while the isotope term agreed with earlier, direct measurements of isotope scattering by Berman and Brock.<sup>24</sup> These parameters were then used for the deformed crystal, adding only the additional scattering caused by the dislocations as calculated from the model of Granato.<sup>15</sup> The results are shown in Fig. 8. The dashed line assumes all phonon modes are scattered with equal strength by dislocations, and assumes the mean dislocation resonance falls at  $\hbar\omega_0/3.8k = 1$  K as suggested by the minimum in  $\kappa T^{-3}$  near  $\approx 0.7$  K. The scattering is too weak to explain the data; decreasing  $\omega_0$  improves agreement below 0.4 K but the scattering then becomes too weak at higher temperatures. If it is assumed that the slow transverse phonons are scattered so strongly that their contribution

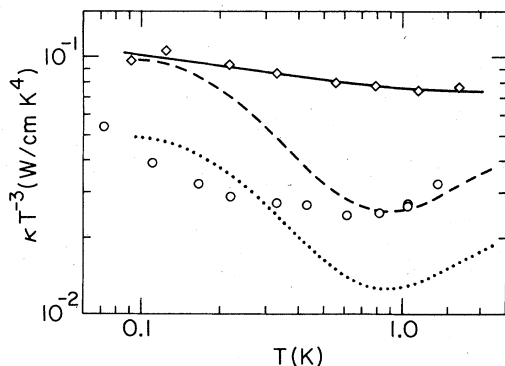


FIG. 8. Thermal conductivity of sample *D* from Fig. 6.  $\diamond$ , undeformed,  $\circ$ , deformed by bending. Solid line, fit to Callaway model with boundary and isotope scattering; dashed and dotted lines, calculations using Callaway model with additional phonon scattering by dislocations as computed from the vibrating-string model. The dashed line assumes all three phonon modes are scattered equally strongly; the dotted curve assumes the slow transverse mode does not contribute to thermal transport because of strong scattering by the dislocations.

to  $\kappa$  may be neglected, and that the other two modes are scattered in accordance with the elastic-string model, the dotted curve is obtained. Now the scattering near 1 K is too strong. Changing  $\omega_0$ , or assuming that the longitudinal mode is also strongly scattered as we suspect, only causes a greater discrepancy between theory and experiment. These are basically the same conclusions as we obtained using the data of Suzuki and Suzuki near 5 K.

In summary, we find that models which associate phonon scattering from dislocations in LiF with static interaction processes are too weak to explain available data over the temperature range 0.03–30 K. The model based on a dynamic interaction with a fluttering dislocation does provide a rough, qualitative explanation for the magnitude of scattering over a limited temperature range near 1 K, and can provide a qualitative explanation for the change in temperature dependence of  $\kappa$  with  $\gamma$  irradiation or annealing. But this dynamic model fails as yet to provide quantitatively the strong mode dependence observed experimentally.

#### D. Some random comments

At temperatures above  $\approx 2$  K, where most data have been obtained for LiF, the temperature dependence is generally closer to  $T^2$  than the  $T^3$  expected from boundary scattering. This temperature dependence is often said to be indicative of a static phonon-dislocation interaction. We believe that the magnitude of the scattering, the temperature dependence, and the change in temperature dependence with thermal treatment<sup>12</sup> are more readily explained by the model of fluttering dislocations.

We emphasize again that only a lower limit of the magnitude of the scattering of slow transverse phonons by dislocations has been observed experimentally, since the fast transverse mode dominates heat flow in the deformed crystal. Only the low-temperature side of a resonant scattering curve can be observed for slow transverse phonons. A portion of this curve is indicated by the squares, for example, near 0.6 K in Fig. 6.

We noted that increasing  $\gamma$  irradiation does not restore  $\kappa$  to its predeformation magnitude for  $T \geq 3$  K. A dislocation resonance at  $\hbar\omega_0/3.8k \geq 3$  K requires the dislocations to have fluttering segments of average length  $\leq 100$  Å. Also the average half-wavelength of the dominate phonons at a temperature of 3 K is  $\approx 100$  Å. It may be that in this regime the concept of pinning or even of an elastic string has begun to fail, and that an atomistic model is more appropriate.

Whereas  $\kappa$  for compressed or bent samples is

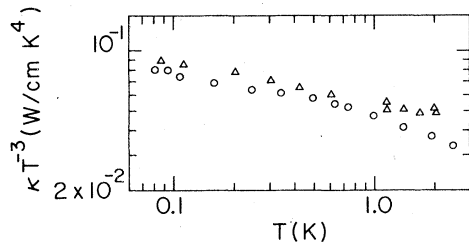


FIG. 9. Thermal conductivities of two bent crystals of  $0.5 \times 0.5$ -cm<sup>2</sup> cross section.  $\Delta$ , thermally annealed in argon at 780° C for 12 h;  $\circ$ , 200 000 R of  $\gamma$  irradiation.

depressed after deformation at all temperatures to  $\approx 25$  K, the  $\kappa$  of a sheared sample appears not to be depressed above  $\approx 10$  K; see Fig. 2. This deformed sample contains a simple array of only edge dislocations and hints that screw dislocations might be responsible for the strong scattering at higher temperatures. However, our data are least reliable at this extreme in temperature; the effect may not be reproducible.

Either annealing or  $\gamma$  irradiation of deformed LiF samples seems to provide the same end product. Figure 9 shows two samples of dimensions  $0.5 \times 0.5 \times 5$  cm<sup>3</sup>, each deformed by bending, one annealed and the other irradiated. At least below  $\approx 1$  K the thermal conductivities are nearly the same. The same behavior is observed for samples deformed by shearing. Annealing causes a reorganization of the dislocations into small-angle boundaries,<sup>3,25</sup> but leaves the number of dislocations essentially unchanged.

Finally, we note that a dynamic phonon-disloca-

tion interaction is not unique to LiF. Evidence for a similar interaction has been obtained in several deformed, superconducting metallic crystals.<sup>26</sup>

#### IV. CONCLUSIONS

All measurements of thermal conductivity and ballistic phonon propagation in deformed LiF crystals are consistent with an interpretation in which the slow transverse (and possibly longitudinal) phonon mode is more strongly scattered by dislocations than the fast transverse mode. Hence fast transverse phonons dominate heat transport at temperature between  $\approx 0.03$  and 25 K. The phonon scattering is too strong to be explained by static mechanisms of phonon-dislocation interaction, but is in rough agreement with calculations based on a resonant or dynamic interaction with dislocations which can flutter in the stress field of passing phonons. The dynamic scattering model can also account for changes in the magnitude and temperature dependence of the thermal conductivity of deformed LiF crystals with  $\gamma$  irradiation or thermal annealing, but the model does not as yet provide the strong scattering dependence determined by phonon mode.

#### ACKNOWLEDGMENTS

This work was supported in part by the Department of Energy under Contract Ey-76-C-02-1198. The authors thank A. V. Granato for helpful discussions and H. S. Ducoff for access to the Cs  $\gamma$  source.

\*Present address: Sandia Laboratories, Albuquerque, New Mexico 87115.

<sup>1</sup>A. C. Anderson and M. E. Malinowski, Phys. Rev. B **5**, 3199 (1972).

<sup>2</sup>Harshaw Chemical Co., Solon, Ohio, 44139.

<sup>3</sup>Additional details are available in the Ph.D. thesis of E. P. Roth (University of Illinois, 1978) (unpublished).

<sup>4</sup>R. J. Soulen, J. F. Schooley, and G. A. Evans, Rev. Sci. Instrum. **44**, 1537 (1973).

<sup>5</sup>A. C. Anderson, R. E. Peterson, and J. E. Robichaux, Rev. Sci. Instrum. **41**, 528 (1970).

<sup>6</sup>M. P. Zaitlin, L. M. Scherr, and A. C. Anderson, Phys. Rev. B **12**, 4487 (1975), and papers cited therein.

<sup>7</sup>R. Berman, F. E. Simon, and J. M. Ziman, Proc. R. Soc. A **220**, 171 (1953).

<sup>8</sup>B. Taylor, H. J. Maris, and C. Elbaum, Phys. Rev. B **3**, 1462 (1971).

<sup>9</sup>L. Kemter and H. Struck, Phys. Status Solidi A **40**, 385 (1977).

<sup>10</sup>A. Taylor, H. R. Albers, and R. O. Pohl, J. Appl. Phys. **36**, 2270 (1965).

<sup>11</sup>R. L. Sproull, M. Moss, and H. Weinstock, J. Appl.

Phys. **30**, 334 (1959); M. Moss, *ibid.* **37**, 4168 (1966).

<sup>12</sup>T. Suzuki and H. Suzuki, J. Phys. Soc. Jpn. **32**, 164 (1972).

<sup>13</sup>Y. Kogure and Y. Hiki, J. Phys. Soc. Jpn. **38**, 471 (1975).

<sup>14</sup>D. Eckhardt and W. Wasserbäch, Philos. Mag. A **37**, 621 (1978).

<sup>15</sup>A. V. Granato, Phys. Rev. **111**, 740 (1958); J. A. Garber and A. V. Granato, J. Phys. Chem. Solids **31**, 1863 (1970).

<sup>16</sup>A. V. Granato and K. Lücke, in *Physical Acoustics*, edited by W. P. Mason (Academic, New York, 1966), p. 225.

<sup>17</sup>T. Ninomiya and S. Ishioka, J. Phys. Soc. Jpn. **23**, 361 (1967); T. Ninomiya, *ibid.* **25**, 830 (1968).

<sup>18</sup>T. Ninomiya, *Treatise on Materials Science and Technology*, edited by H. Herman (Academic, New York, 1975) Vol. 8, p. 1.

<sup>19</sup>An exponential distribution of segment lengths is assumed. See Ref. 15 and papers cited therein.

<sup>20</sup>K. Ohashi and Y. H. Ohashi, Philos. Mag. A **38**, 187 (1978).

<sup>21</sup>A. V. Granato (private communication). The mass term takes the form  $\rho b^2/4\pi$  in  $\Theta_D/T$ , which is more appropriate to the high frequencies involved in thermal measurements than the form  $\rho b^2$  used at ultrasonic frequencies. The line tension is assumed to have the same functional dependence, hence the ratio of mass to line tension is unchanged.

<sup>22</sup>M. Peach and J. S. Koehler, Phys. Rev. 80, 436 (1950).

<sup>23</sup>J. Callaway, Phys. Rev. 113, 1046 (1959).

<sup>24</sup>R. Berman and J. C. F. Brock, Proc. R. Soc. A 289, 46 (1965).

<sup>25</sup>E. P. Roth and A. C. Anderson, Phys. Rev. B 17, 3356 (1978).

<sup>26</sup>S. G. O'Hara and A. C. Anderson, Phys. Rev. 9, 3730 (1974); 10, 574 (1974).